WATER RESOURCES RESEARCH, VOL. 36, NO. 12, PAGES 3567–3580, DECEMBER 2000

A fast algorithm for the estimation of the equivalent hydraulic conductivity of heterogeneous media

Philippe Renard,[1,2] Gaëlle Le Loc'h,[3] Emmanuel Ledoux,[1] Ghislain de Marsily,[4] and Rae Mackay[5]

Abstract. Fast upscaling of hydraulic conductivity is a recurrent problem in modeling flow through heterogeneous porous media. We propose a new renormalization technique. It is based on the iterative application of the *Cardwell and Parsons* [1945] bounds on elementary groups of cells. The combination of the bounds with a heuristic formula allows anisotropy to be taken into account. The new technique is tested and compared with other fast techniques. Among the tested techniques the two most reliable ones are the tensorial renormalization and the new simplified renormalization. The numerical efficiency of the simplified renormalization leads us to recommend it when a diagonal tensor of equivalent conductivity is sufficient.

1. Introduction

Modeling groundwater flow and transport requires a realistic description of the spatial distribution of hydraulic conductivity to capture flow paths and to make realistic forecasts of groundwater behavior. As discussed by *de Marsily et al*. [1998] and *Koltermann and Gorelick* [1996], statistical and genetic tools can be used to describe the underground distribution of hydraulic conductivity. Geological models generated by these tools often produce a very high spatial resolution which cannot be used directly in groundwater flow and transport models given currently available computer resources. It is necessary to adopt a much coarser description. This upscaling comprises the calculation of spatial averages of the hydraulic conductivity over blocks of the geological model that can be used directly in the groundwater model. This problem is different from the problem of finding a unique effective conductivity for the whole aquifer. *Renard and de Marsily* [1997] and *Wen and Gómez-Hernández* [1996] present extensive reviews of upscaling theories, analytical results, and numerical techniques.

In this paper, we develop a fast real-space renormalization algorithm to calculate block conductivities. The essence of renormalization is to apply composition rules to groups of cells at the local scale to produce "composite" cells and then to successively reapply the same rules to the resulting composite cells until the desired coarse-scale resolution is achieved. The basic assumption is that the upscaling rules are scale invariant. When the probability distribution of the local-scale conductivity is known, it is possible to follow the evolution of the probability distribution of hydraulic conductivity with scale. This approach was initially developed in the field of physics [*Wilson*, 1971, 1975; *Reynolds et al*., 1977; *Bernasconi*, 1978; *Shah and Ottino*, 1986]. Recently, real-space renormalization has been applied to a broad range of problems related to the physics of groundwater in porous and fractured media [*King*, 1989; *Aharony et al*., 1991; *Saucier*, 1992; *King et al*., 1993; *Hinrichsen et al*., 1993; *Zimmerman and Bodvarsson*, 1996; *Gautier and Nœtinger*, 1997; *Xu et al*., 1997; *Jaekel and Vereecken*, 1997; *Hansen et al*., 1997; *Gavrilenko and Guéguen*, 1998]. We do not consider the probabilistic aspect of renormalization group theories, but, instead, we focus our work on the spatial averaging scheme. Previous schemes [*King*, 1989; *Hinrichsen et al*., 1993; *Gautier and Nœtinger*, 1997] solve a flow problem on the elementary groups of cells at the local scale by fixing the boundary conditions of the groups. Our approach is different and is based on applying *Cardwell and Parsons* [1945] bounds iteratively. At the end of the iteration process we obtain two values more closely spaced than the bounds that would be obtained by direct calculation on the full mesh, and we average these with a heuristic formula based on the analytical development of *Romeu* [1994].

Renormalization algorithms are computationally efficient but subject to approximation errors. The major aim of our research is to investigate possible errors and to compare the renormalization schemes with a set of other fast techniques. The comparison is based on a very large number of numerical experiments conducted on synthetic media at two different scales. This approach was pioneered by *Warren and Price* [1961] and followed by many researchers [*Desbarats*, 1987; *Le Loc'h*, 1987; *Deutsch*, 1989; *Ababou et al*., 1989; *Gómez-Hernández*, 1991; *Lachassagne et al*., 1990; *Bachu and Cuthiell*, 1990; *Hinrichsen et al*., 1993; *Desbarats*, 1992; *Sànchez-Vila et al*., 1995; *McCarthy*, 1995]. The synthetic media were generated by truncated Gaussian and Boolean methods with strong anisotropy in both cases. They represent a priori nontrivial situations for the upscaling problem.

For each medium a reference block conductivity is calculated by solving numerically the usual Laplace flow equation using finite element or finite difference methods. This step provides reference values to compare the upscaling techniques. It is important to recall that *Lachassagne et al*. [1990] and later

[1]Centre d'Informatique Géologique, Ecole des Mines de Paris, Fontainebleau, France.
[2]Now at Swiss Federal Institute of Technology, Institute of Geology, Zürich, Switzerland.
[3]Centre de Géostatistique, Ecole des Mines de Paris, Fontainebleau, France.
[4]Laboratoire de Géologie Appliquée, Université Pierre et Marie Curie, Paris.
[5]School of Earth Science, University of Birmingham, Birmingham, England.

Paper number 2000WR900203.
0043-1397/00/2000WR900203$09.00

Romeu and Nœtinger [1995] have shown that such reference values are in general significantly biased. *Lachassagne et al*. [1990] showed that for a lognormal two-dimensional medium, finite element techniques overestimate the conductivity, while finite difference techniques give different biases that depend on the intermesh averaging rule. With the usual harmonic averaging rule, finite differences underestimate the equivalent conductivity. In all cases, *Lachassagne et al*. [1990] showed that the problem can be solved by overdiscretizing the mesh; each cell of constant conductivity has to be discretized in subelements. However, the level of required overdiscretization is generally difficult to predict. It depends on the degree of heterogeneity, the correlation structure of the heterogeneous media, and the numerical scheme. Historically, this has led to a series of wrong conclusions when researchers have compared numerical results with analytical formulae. The reader is referred to *Romeu* [1994] for a more detailed discussion. In this work, the use of both finite element and finite difference techniques, without solving this difficulty, allowed a check on whether or not the comparison was dependent on the numerical bias.

2. Fast Techniques

A fairly complete review of past research in the area of upscaling has been conducted [*Renard and de Marsily*, 1997]. The following seven methods were selected and compared with the proposed simplified renormalization.

2.1. Arithmetic μ_a and Harmonic μ_h Means

The arithmetic μ_a and harmonic μ_h means are the upper and the lower bound for upscaled permeability, respectively [*Wiener*, 1912; *Cardwell and Parsons*, 1945; *Matheron*, 1967; *Le Loc'h*, 1987; *Dagan*, 1989]. They are the exact values in the case of a stratified medium with flow respectively parallel or perpendicular to the strata.

2.2. Geometric Mean μ_g

The geometric mean μ_g is the exact upscaled value in an infinite two-dimensional medium, if the normalized local permeabilities $k/E(k)$ and their inverses $k^{-1}/E(k^{-1})$ have the same probability density function (pdf), if this pdf is invariant by rotation of 90° and if the flow is uniform [*Matheron*, 1967]. This is true in the cases of a chessboard and of a lognormal isotropic medium. In practice, it can be considered as a good effective value in two dimensions, even in radial flow conditions [*Meier et al*., 1998].

2.3. Landau-Lifshitz-Matheron Conjecture $\mu_{1/3}$

Landau and Lifshitz [1960] in the framework of electrodynamics, and *Matheron* [1967] in the context of uniform flow through porous media, made the conjecture that the first-order approximation of the effective conductivity of a three-dimensional isotropic heterogeneous medium would be

$$K_{ef} = \mu_a^{2/3}\mu_h^{1/3}. \tag{1}$$

An alternative equivalent expression for this conjecture is a power average with an exponent of one third [*Nœtinger*, 1994]:

$$K_{ef} = \mu_{1/3} = \left(\frac{1}{V} \int_V k(\mathbf{x})^{1/3}\, d\mathbf{x} \right)^3, \tag{2}$$

where V is the averaging volume, k is the local-scale conductivity, and $\mathbf{x}$ is the spatial coordinate. This conjecture has been the subject of intensive research [*Gutjahr et al*., 1978; *Gelhar and Axness*, 1983; *King*, 1987; *Dagan*, 1993; *Kozlov*, 1993; *Nœtinger*, 1994; *Abramovich and Indelman*, 1995; *De Wit*, 1995; *Teodorovich*, 1997; *Pozdniakov and Tsang*, 1999]. Numerical experiments have shown a good agreement with the conjecture for lognormal media even for high variances [*Dykaar and Kitanidis*, 1992; *Desbarats*, 1992; *Neuman and Orr*, 1993] even if the latest analytical developments [*Abramovich and Indelman*, 1995; *De Wit*, 1995; *Teodorovich*, 1997] indicate that the conjecture is only an approximation.

2.4. Romeu's Formula k_r

Following the idea that the actual conductivity of a heterogeneous medium can be obtained by averaging theoretical bounds with an adequate procedure, one possibility is to use some bounds which are closer than the arithmetic mean and the harmonic mean and then to average them. Whatever the averaging procedure, the closer the bounds are, the smaller the expected errors are.

Duquerroix et al. [1993] and *Romeu* [1994] proposed such a technique using the *Cardwell and Parsons* [1945] bounds. Recall that *Cardwell and Parsons* [1945] and *Le Loc'h* [1987] showed that the equivalent permeability for a uniform flow in a given direction is bounded by (1) the harmonic mean of the arithmetic means of the local permeabilities, calculated over each slice of cells perpendicular to the given direction (upper bound denoted K_1),

$$K_1 = \mu_h^x(\mu_a^y(\mu_a^z)) = \mu_h^x(\mu_a^z(\mu_a^y)) = \frac{n_x}{n_y n_z}\left[\sum_{i=1}^{n_x} \left(\sum_{j=1}^{n_y} \sum_{k=1}^{n_z} k_{i,j,k}^{xx} \right)^{-1} \right]^{-1}, \tag{3}$$

and (2) the arithmetic mean of the harmonic means of the local permeabilities, calculated on each line of cells parallel to the given direction (lower bound denoted K_2),

$$K_2 = \mu_a^y(\mu_a^z(\mu_h^x)) = \mu_a^z(\mu_a^y(\mu_h^x)) = \frac{n_x}{n_y n_z} \sum_{j=1}^{n_y} \sum_{k=1}^{n_z} \left[\sum_{i=1}^{n_x} (k_{i,j,k}^{xx})^{-1} \right]^{-1}. \tag{4}$$

Le Loc'h [1987] proposed to take the geometric average of these bounds $K_b = \sqrt{K_1 K_2}$. *Lemouzy* [1991] introduced, in three dimensions, two intermediate values K_3 and K_4 into the formula:

$$K_3 = \mu_a^y(\mu_h^x(\mu_a^z)), \tag{5}$$

$$K_4 = \mu_a^z(\mu_h^x(\mu_a^y)), \tag{6}$$

$$K_b = \sqrt[6]{(K_1)^2(K_2)^2 K_3 K_4}. \tag{7}$$

Finally, *Romeu* [1994] and *Duquerroix et al*. [1993] introduced an exponent to account for anisotropy:

$$k_r^{xx} = K_1^{(\theta_{y2}\theta_{z3}+\theta_{z2}\theta_{y3})} K_2^{(1-\theta_{y3}-\theta_{z3})} K_3^{(1-\theta_{z2})\theta_{y3}} K_4^{(1-\theta_{y2})\theta_{z3}}. \tag{8}$$

The exponents are derived from a small perturbation calculation of the equivalent permeability in the case of an anisotropy due to flat cells and/or to a constant anisotropy of directional permeability in the domain [*Romeu*, 1994]:

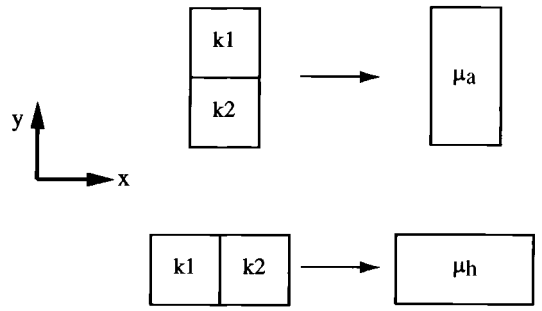

Figure 1. Local formula to calculate the upscaled permeability for a group of two cells. It is the arithmetic mean μ_a when they are in parallel and the harmonic mean μ_h when they are in series.

$$\theta_{y2} = \frac{\arctan \sqrt{a_y}}{\pi/2}, \tag{9}$$

$$\theta_{z2} = \frac{\arctan \sqrt{a_z}}{\pi/2}, \tag{10}$$

$$\theta_{y3} = \frac{\theta_{y2}(1 - \theta_{z2})}{1 - \theta_{y2}\theta_{z2}}, \tag{11}$$

$$\theta_{z3} = \frac{\theta_{z2}(1 - \theta_{y2})}{1 - \theta_{y2}\theta_{z2}}; \tag{12}$$

a_y and a_z are the anisotropy factors defined by

$$a_y = (k^{yy}/k^{xx})(d_x/d_y)^2 \tag{13}$$

$$a_z = (k^{zz}/k^{xx})(d_x/d_z)^2, \tag{14}$$

where d_x, d_y, and d_z represent the size of the cells and the local conductivity anisotropy ratios k^{yy}/k^{xx} and k^{zz}/k^{xx} which are assumed to be constant over the whole mesh. An alternative empirical technique to average the *Cardwell and Parsons* [1945] bounds has been proposed by *Li et al*. [1999] but has not been studied here.

2.5. Standard Renormalization r_s

We call the algorithm proposed by *King* [1989] standard renormalization. The upscaled permeability is calculated by a series of successive aggregations on elementary groups of four (in two dimensions) or eight (in three dimensions) cells following an electrical analogy. This electrical analogy is equivalent to a finite difference calculation with intermesh transmissivities calculated with a harmonic mean and with prescribed boundary conditions of constant head on two opposite faces and no flow on the other faces.

2.6. Tensorial Renormalization r_t

The tensorial renormalization was developed for the fast detection of preferential flow paths in heterogeneous media [*Gautier and Nœtinger*, 1997]. The differences from the standard algorithm are the use of a "direct" finite element scheme avoiding the calculation of intermesh transmissivities and the use of periodic boundary conditions that allow the calculation of a complete conductivity tensor. We extended the equations of *Gautier and Nœtinger* [1997] in three dimensions.

3. Simplified Renormalization

The simplified renormalization algorithm allows the estimation of a diagonal tensor of hydraulic conductivity. We describe the algorithm for the estimation of k^{xx}. The procedure is the same for the other directions.

In the first step we group the cells alternatively in parallel and in series with respect to the direction of calculation. If the two cells are in series, they are replaced by a unique cell whose conductivity is the harmonic mean $\mu_h = 2k_1k_2/(k_1 + k_2)$ of the conductivity of the cells (Figure 1). If the two cells are in parallel, we use the arithmetic mean $\mu_a = (k_1 + k_2)/2$ (Figure 1). This basic procedure is systematically repeated until we get a unique value. The order of grouping influences the final result. In two dimensions (Figure 2) we can start with a grouping in series along the x direction, then we group the new pairs in parallel along the y direction, then we repeat this basic algorithm until we get a value that we denote $c^{xx}_{\min}$, represented by

$$c^{xx}_{\min} = \mu^y_a(\ \ldots\ \mu^y_a(\mu^x_h)\ \ldots\ ). \tag{15}$$

Alternatively, we can start with a grouping in parallel along the y direction, then we group the new pairs in series along the x direction, then we repeat the algorithm to get a value denoted $c^{xx}_{\max}$:

$$c^{xx}_{\max} = \mu^x_h(\ \ldots\ \mu^x_h(\mu^y_a)\ \ldots\ ). \tag{16}$$

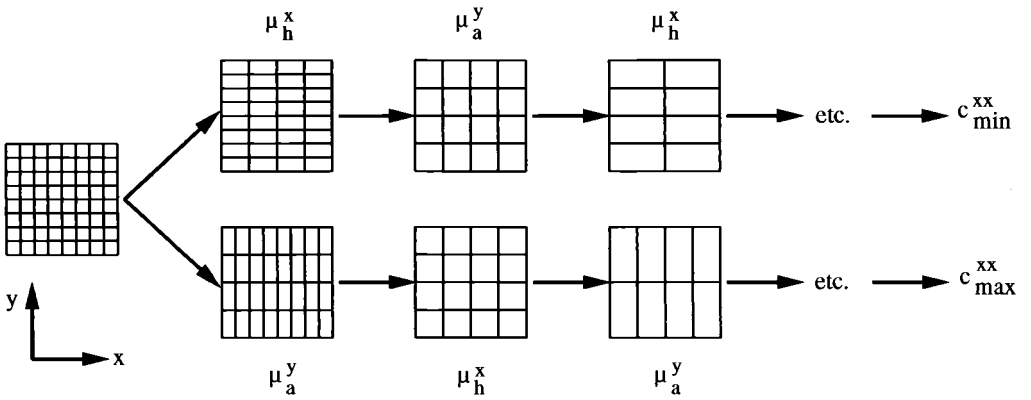

Figure 2. Simplified renormalization procedure in two dimensions. The cells are grouped two by two iteratively in order to finally obtain two values denoted $c_{\min}$ and $c_{\max}$.

Table 1. Number of Small Blocks

Model	Number of Small Blocks
Boolean ellipsoidal inclusion	18,432
Boolean sinusoidal inclusion	6,144
Truncated Gaussian short range	2,560
Truncated Gaussian long range	40,448
Total	67,584

In three dimensions, there are four possibilities:

$$c^{xx}_{\min} = \mu^y_a(\ \ldots\ \mu^y_a(\mu^z_a(\mu^x_h))\ \ldots\ ) = \mu^z_a(\ \ldots\ \mu^z_a(\mu^y_a(\mu^x_h))\ \ldots\ ), \tag{17}$$

$$c^{xx}_{\max} = \mu^x_h(\ \ldots\ \mu^x_h(\mu^z_a(\mu^y_a)\ \ldots\ ) = \mu^x_h(\ \ldots\ \mu^x_h(\mu^y_a(\mu^z_a))\ \ldots\ ), \tag{18}$$

$$c^{xx}_3 = \mu^y_a(\ \ldots\ \mu^y_a(\mu^x_h(\mu^z_a))\ \ldots\ ), \tag{19}$$

$$c^{xx}_4 = \mu^z_a(\ \ldots\ \mu^z_a(\mu^x_h(\mu^y_a))\ \ldots\ ). \tag{20}$$

In general, $c_{\min}$ and $c_{\max}$ are different; $c_{\min}$ is always smaller than or equal to $c_{\max}$. This is not surprising because we calculated the *Cardwell and Parsons* [1945] bounds on each elementary group of cells. It is therefore expected that the true conductivity of the medium is between $c_{\max}$ and $c_{\min}$. Note that (1) the difference between $c_{\max}$ and $c_{\min}$ is smaller than the difference between the Cardwell and Parsons bounds, and (2) there is no theoretical proof that $c_{\max}$ and $c_{\min}$ are actual bounds of the equivalent hydraulic conductivity. We have not used the values c_3 and c_4.

In the case where the cells are not of the same size and their conductivity is not isotropic, the equivalent conductivity of the pair of cells can be calculated with the analytical formula provided by *Quintard and Whitaker* [1987, equation 3.36]. We have not applied this, but the final equivalent conductivity would be a full tensor.

The anisotropy due to the spatial structure of the distribution of the hydraulic conductivity is taken into account by the iterative procedure described above. Another kind of anisotropy arises when the grid cells are not cubic but are flattened. In this case we propose a formula to estimate K_b as a combination of $c_{\min}$ and $c_{\max}$, taking into account the anisotropy due to the flattening of the cells. We use the classical technique of an exponent varying between 0 and 1:

$$K^{ii}_b \approx c^{ii} = (c^{ii}_{\max})^{\alpha}(c^{ii}_{\min})^{1-\alpha} \qquad \alpha \in [0,\ 1] \quad i \in \{x, y, z\}. \tag{21}$$

The anisotropy ratio due to flat cells is defined as

$$a^i_j = (d_i/d_j)^2 \qquad (i, j) \in \{x, y, z\}^2, \tag{22}$$

Table 2. Sets of Ranges for the Covariance Models

	Horizontal Range, cells	Vertical Range, cells
a1	8	5
a2	50	5
a3	50	15

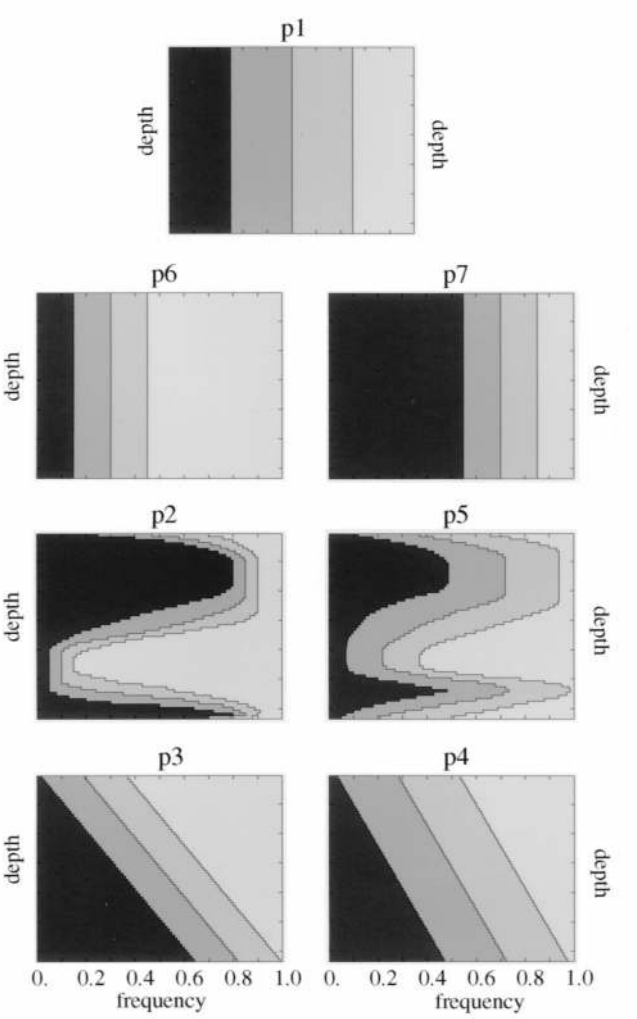

Figure 3. The seven curves of proportion of lithofacies as a function of depth used to generate the truncated Gaussian media. Sets p1, p6, and p7 show constant proportions with depth. The others show varying proportions with depth.

where d_i and d_j represent the size of the cells in directions i and j. The numerical experiments presented below (Plate 1) suggest that K^{xx}_b tends toward $c^{xx}_{\min}$ when the cells are flattened along the x direction (a^x_z and a^x_y tending toward 0), while K^{xx}_b tends toward $c^{xx}_{\max}$ when the cells are flattened in one of the other directions. We propose therefore to modify (8) developed by R. K. Romeu by postulating that there are only two asymptotic values ($c^{xx}_{\max}$ and $c^{xx}_{\min}$) for the conductivity instead of three [*Duquerroix et al.*, 1993, equations 25, 26, and 27]. The composition formula is simplified according to this postulate, and we get

$$c^{ii} = (c^{ii}_{\max})^{\alpha}(c^{ii}_{\min})^{1-\alpha} \tag{23}$$

with α, expressed as a function of the anisotropy ratios a^i_j and a^i_k:

$$\alpha(a^i_j,\ a^i_k) = \frac{u(a^i_j) + u(a^i_k) - 2u(a^i_j)u(a^i_k)}{1 - u(a^i_j)u(a^i_k)}, \tag{24}$$

$$(i, j, k) \in \{x, y, z\}^3 \qquad i \neq j \neq k$$

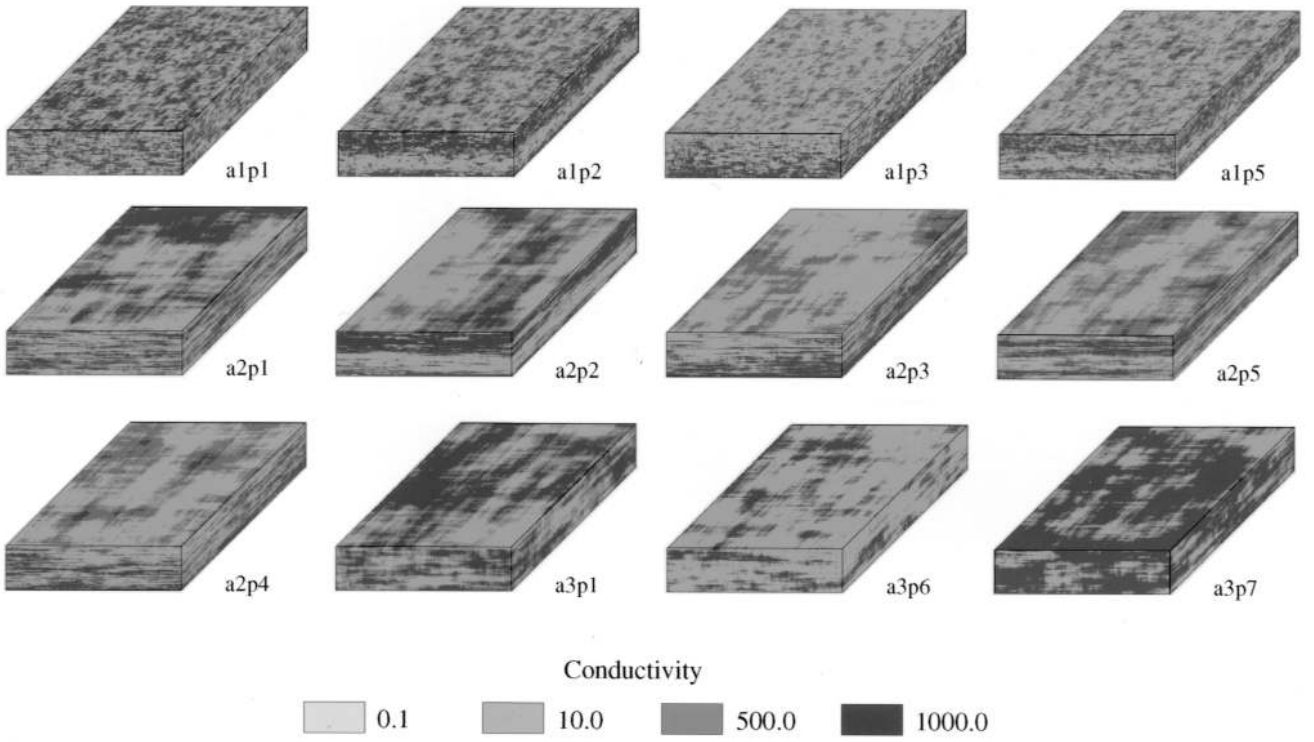

Figure 4. One example of each kind of the truncated Gaussian media. Some are statistically homogeneous (i.e., the type a1p1), but most of them are nonstationary due either to large correlation structures compared to the size of the domain (i.e., a2p1) or to trends in the proportions of the facies with depth (i.e., a1p2), or both (a2p2).

$$u(t) = \frac{\arctan \sqrt{t}}{\pi/2}. \tag{25}$$

4. Synthetic Conductivity Fields and Reference Values

To test the fast upscaling rules, 1966 hydraulic conductivity fields were generated on regular grids with $128 \times 128 \times 64$ ($\approx$1 million) cells. The cells are flattened and have a size of $10 \times 10 \times 1$ units. Thirty-two realizations were generated for each parameter set. To investigate the effect of block size on the upscaling techniques, we extracted 67,584 small blocks ($16 \times 16 \times 8 = 2048$ cells) from these large blocks (see Table 1). We now describe the models and parameters used to generate these media.

4.1. Truncated Gaussian Media

The truncated Gaussian media were generated with the HERESIM software (Institut Français du Pétrole/Ecole des Mines de Paris). The model operates by simulating a Gaussian function and truncating it to obtain a discrete variable: the lithofacies [*Matheron et al*., 1987]. The parameters are a covariance function and the proportions of the different lithofacies. We used four facies, a factorized exponential model of covariance with three different sets of ranges a1 to a3 (Table 2). For the proportions, seven sets p1 to p7 of parameters were used (Figure 3). Sets p1, p6, and p7 have constant proportions along the depth. For p1 the four facies are equally represented. For p6 the proportion of facies 1, 2, 3, and 4 are 0.15, 0.15, 0.15, and 0.55 respectively, while for the set p7 they are 0.55, 0.15, 0.15, and 0.15, respectively. For the sets p3 and p4 the proportions vary linearly with depth. For the set p4 the global proportions over the whole domain are 0.25 for all the facies. For the sets p2 and p5 the proportions are defined in the order that layers with predominating facies are generated. Thirteen combinations of covariance and proportions were used: a1p1, a1p2, a1p3, a1p4, a1p5, a2p1, a2p2, a2p3, a2p4, a2p5, a3p1, a3p6, and a3p7. In the last step a conductivity is assigned to each facies: For lithofacies 1, 2, 3, and 4, conductivities k are 1000, 500, 10, and 0.1, respectively. Figure 4 shows one realization of such media for each set of parameters.

4.2. Boolean Media

The Boolean model [*Matheron*, 1967; *Haldorsen and Damsleth*, 1990] generates points in three-dimensional space according to a Poisson process and assigns to each point an inclusion whose size, orientation, and shape follow predefined probability functions. The parameters are the density of the Poisson process, which is related to the total number of inclusions, the shape of the inclusions, and the parameters of size and orientation of the inclusions. We used five different densities named b1 to b5, four different types of elliptical inclusions e1 to e4, and two different types of sinusoidal inclusions s1 and s2. Finally, we have eight sets of parameters b1e1, b2e2, b1e3, b3e3, b4e4, b5e4, b1s1, and b2s2. Figure 5 shows one realization for each set of parameters. To enlarge the domain of investigation, for each realization, we used six different pairs of conductivity values for the inclusion and the matrix (Table 3).

4.3. Reference Block Conductivity

The equivalent conductivity (or block conductivity) of any heterogeneous block was calculated following the same ap-

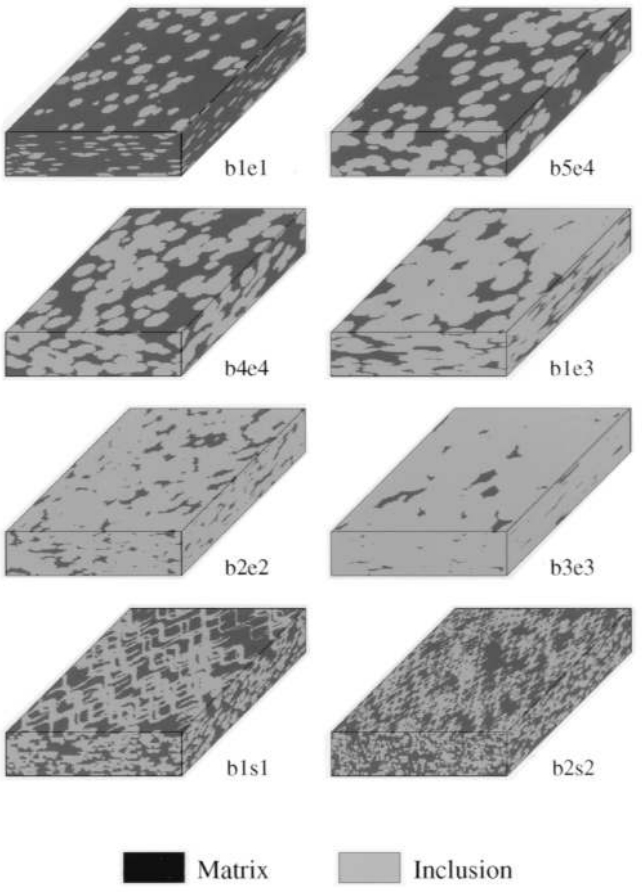

Figure 5. One example of each type of the Boolean media. The differences are due to the density, the size, and the shape of the inclusions.

proach as past workers such as *Warren and Price* [1961] and others. We used the multigrid finite element code TRIMULEC [*Goblet*, 1992] to solve the groundwater flow equation in steady state with permeameter-type boundary conditions (Figure 6). Three calculations, with a rotation of the boundary conditions, were conducted to obtain the directional conductivities.

The use of permeameter-type boundary conditions is justified since the principal axes of anisotropy are parallel to the axes of the grid. This has been checked numerically by calculating the full tensor of equivalent conductivity on some representative cases and comparing the results with the approach described in the previous paragraph. The differences between the diagonal components of the conductivity tensor were less than 1% in all the tested cases, and the off-diagonal terms were between 1 and 3 orders of magnitude lower than the diagonal terms [*Renard*, 1997].

To investigate the effect of the numerical bias (on at least one large block for each parameter set), we did the same

Table 3. Conductivity Couples Used for the Boolean Media

Name	1	2	3	4	5	6
k matrix	100	100	100	0.1	1	10
k inclusion	0.1	1	10	100	100	100

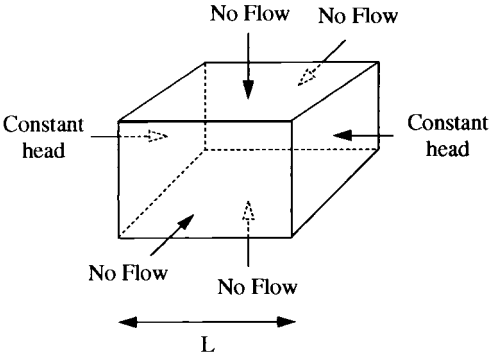

Figure 6. Schematic diagram of the permeameter-type boundary conditions imposed on the block to calculate the equivalent hydraulic conductivity.

calculations with the finite difference code HIGHDEN developed at the University of Newcastle. HIGHDEN was not applied to the small blocks. The difference between the results obtained with TRIMULEC and HIGHDEN is around 5% on average but can reach 30% for the estimation of the vertical conductivity. These differences indicate that we must compare the fast techniques with both references.

5. Criteria of Classification of the Fast Upscaling Techniques

For all the media we have at least one reference value and one block conductivity for each fast upscaling technique. The most general way to compare the results of a set of values with reference values is to study the scatter diagrams of these pairs of values. However, to rank the techniques we also need numerical criteria. The first one is the relative bias: the ratio of the mathematical expectation (experimentally, the average) of the error and the expectation of the reference value,

$$e = \frac{\left| \sum_i (Y^i_{\text{ref}} - Y^i_{\text{quick}}) \right|}{\sum_i Y^i_{\text{ref}}}, \tag{26}$$

where i is an index over all the synthetic conductivity fields, $Y^i_{\text{ref}} = \log_{10} K^i_{\text{ref}}$ is the reference value for the ith synthetic medium, and Y^i_{quick} is the estimation of the upscaled conductivity with a given quick technique. The parameter e is calculated on the logarithm of the conductivity, because the order of magnitude is more important than the value itself.

The bias itself is not sufficient because large positive and negative errors can be averaged in such a way that the bias is small although the estimation is inaccurate. To quantify the dispersion, we need another criterion. We used the linear correlation coefficient:

$$\rho = \frac{\sum_i (Y^i_{\text{ref}} - \bar{Y}_{\text{ref}})(Y^i_{\text{quick}} - \bar{Y}_{\text{quick}})}{\sqrt{\sum_i (Y^i_{\text{ref}} - \bar{Y}_{\text{ref}})^2} \sqrt{\sum_i (Y^i_{\text{quick}} - \bar{Y}_{\text{quick}})^2}}, \tag{27}$$

where $\bar{Y}$ represents the mean over all the media, i.e., $\bar{Y} = 1/n \, \Sigma_{i=1}^n Y^i$. A value of ρ around 1 indicates a small dispersion around a linear relation between the two variables. Using such

Table 4. Comparison of the Classification of the Upscaling Techniques When Finite Elements or Finite Differences Are Used as the Reference Value[a]

	K_b^{zz}						K_b^{xx}					
	Finite Elements			Finite Differences			Finite Elements			Finite Differences		
Rank	Method	ρ	e	Method	ρ	e	Method	ρ	e	Method	ρ	e
1	r_t	0.975	0.316	r_t	0.945	0.340	r_t	0.997	0.030	r_t	0.999	0.014
2	r_s	0.973	0.287	r_s	0.941	0.314	c	0.997	0.019	c	0.998	0.002
3	c	0.968	0.330	c	0.934	0.357	k_r	0.996	0.014	k_r	0.995	0.003
4	k_r	0.765	0.693	k_r	0.802	0.687	r_s	0.989	0.067	r_s	0.995	0.051
5	μ_g	0.666	0.488	μ_g	0.710	0.518	μ_a	0.981	0.048	μ_a	0.978	0.066
6	μ_h	0.507	1.206	μ_h	0.530	1.21	$\mu_{1/3}$	0.972	0.144	$\mu_{1/3}$	0.975	0.130
7	$\mu_{1/3}$	0.399	1.209	$\mu_{1/3}$	0.438	1.25	μ_g	0.725	0.424	μ_g	0.736	0.414
8	μ_a	0.155	1.705	μ_a	0.188	1.76	μ_h	−0.303	1.080	μ_h	−0.283	1.081

[a]The classification is based on the comparison of K_b of the 612 large blocks for which we computed the reference value both with TRIMULEC and HIGHDEN. Abbreviations are as follows: r_t, tensorial renormalization; r_s, standard renormalization; c, simplified renormalization; k_r, Romeu's formula; μ_g, geometric mean; μ_h, harmonic mean; $\mu_{1/3}$, Landau-Lifshitz-Matheron conjecture; and μ_a, arithmetic mean.

a criterion does not allow detection of nonlinear relations between the variables, but we are not interested in these kinds of relations. We need to find the techniques that give directly the best estimation of the reference value, and we do not want to have to apply an additional empirical correction to the result of the quick technique.

To visually summarize the classification using both the relative bias and the correlation coefficient, we represent the results of the different upscaling techniques in a quality plot: A point corresponds to a technique, and its coordinates are the relative bias and the correlation coefficient. The closer the point is to the upper left-hand corner ($e = 0$, $\rho = 1$), the more accurate the technique is. For a technique to be reliable, it must stay in this upper left-hand corner when the conditions of the test are changed.

6. Results

6.1. Effect of the Reference Value

Table 4 shows that the classification of the upscaling techniques remains identical even if the values for the bias and for the correlation coefficient are different when we use a reference value calculated with TRIMULEC or HIGHDEN. In the following we will discuss only the classification obtained by using the reference values calculated with TRIMULEC for which the largest number of simulations was done.

6.2. Scatter Diagrams

In each scatter diagram the conductivities calculated with the fast technique are plotted along the abscissa, and the reference conductivities calculated with TRIMULEC are plotted along the ordinate. The better the technique is, the closer are all the points from the bisector $y = x$. Because of the importance of anisotropy and block size the results for K^{xx} and K^{zz} and the results for the large blocks and for the small blocks are plotted separately. We do not present the plots for K^{yy} because they are almost identical to those of K^{xx}.

Plate 1 shows the scatter diagrams that allow the comparison of the Cardwell and Parsons bounds with $c_{\max}$ and $c_{\min}$ for all block sizes and flow directions. We observe that in accordance with the theory, K_1 and K_2 always bound the reference value whatever the size of the blocks and the flow direction. Values $c_{\max}$ and $c_{\min}$ are closer to the bisector line than K_1 and K_2, implying that they are closer to the reference values. However, $c_{\max}$ and $c_{\min}$ do not bound the reference conductivities as the cloud of points is not bounded by the bisector line. Furthermore, (as mentioned in section 3), the anisotropy causes $c_{\max}$ to tend toward the reference values for flow in the x direction for large and small blocks (Plates 1c and 1k), while $c_{\min}$ tends toward the reference for flow in the z direction for large and small blocks (Plates 1h and 1p).

Plate 2 shows the scatter diagrams that allow an analysis of which fast upscaling techniques are the most accurate for large blocks. Plate 3 shows the same diagrams for the small blocks. A visual check of these scatter diagrams shows that no technique gives a good estimation of the conductivity in the z direction for the large blocks (Plates 2i–2p). Better results are obtained in the x direction for large blocks (Plates 2a–2h) and in all directions for the small blocks (Plate 3). In Plates 2 and 3 the scatter diagrams corresponding to algebraic means (μ_h, μ_a, μ_g, and $\mu_{1/3}$) are always more scattered and more distant from the bisector and therefore less accurate than those corresponding to the renormalization schemes (c, r_s, and r_t) or to Romeu's formula k_r.

In Plates 2 and 3 the color of the dot corresponds to the type of medium: red is truncated Gaussian with a long correlation range; dark blue is truncated Gaussian with a small correlation range; green is Boolean media with ellipsoidal inclusions; and light blue is Boolean media with sinusoidal inclusions. This color coding shows that some techniques can give good estimations for a specific type of medium, while they are not accurate for another type. For example, the geometric mean gives an acceptable estimation of the vertical conductivity of Boolean media, while it is not acceptable for truncated Gaussian media (Plate 2k). The color coding also shows that for the Boolean media some nonlinear relations exist between the harmonic mean and the equivalent hydraulic conductivity (Plate 2a). Note, however, that our goal is not to study this type of relation.

6.3. Efficiency of the Techniques

Table 5 shows the mean CPU time for each upscaling technique and the time for full solution using the finite element method. The standard renormalization is slower than the tensorial renormalization technique because it has to solve a linear system 3 times, and the tensorial renormalization has to solve only one linear system. The simplified renormalization does not involve the solution of a linear system of equations

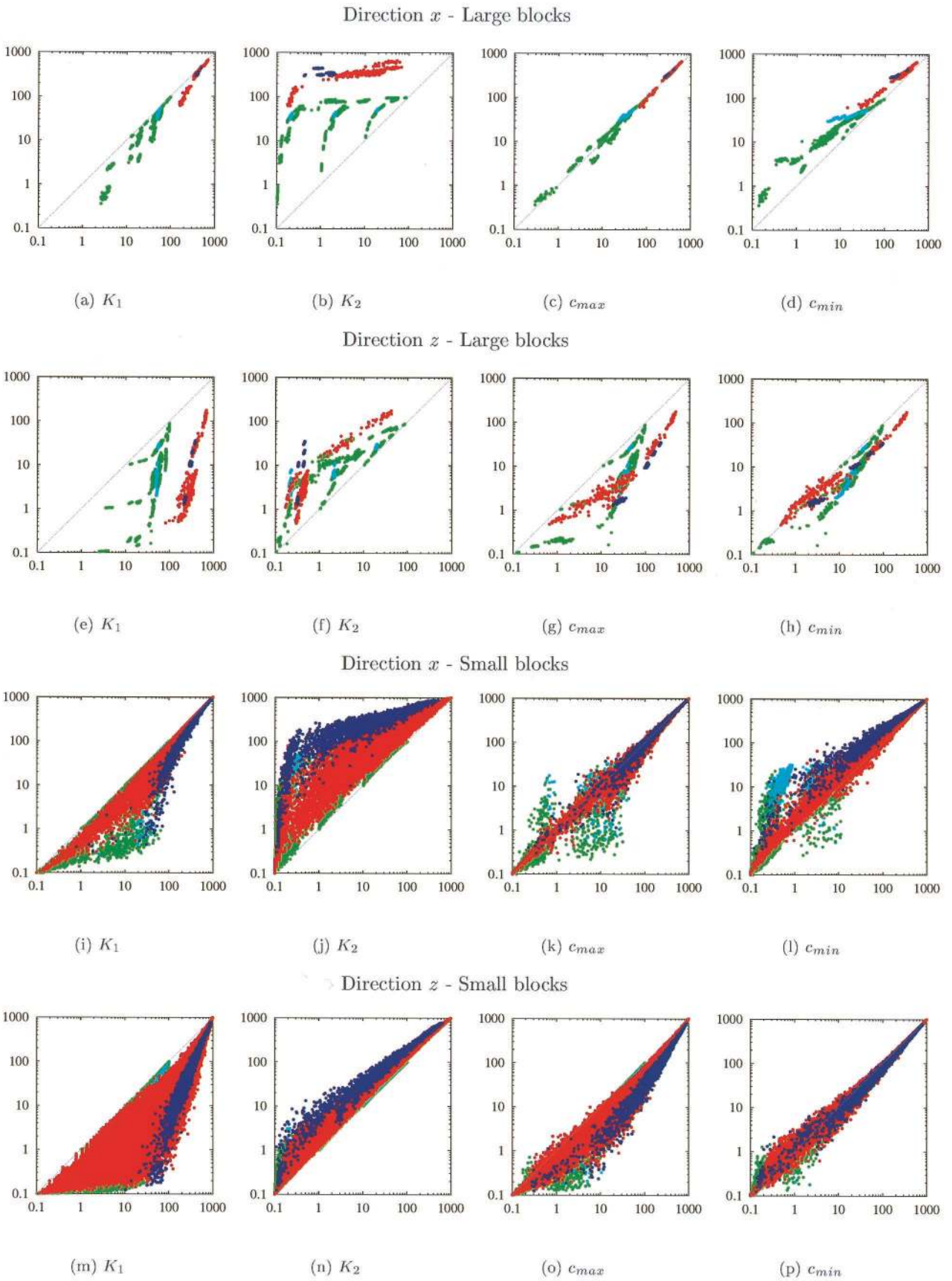

Plate 1. Scatter diagrams showing the reference equivalent conductivity (ordinate) calculated with finite elements as a function of the *Cardwell and Parsons* [1945] upper bound K_1 and lower bound K_2 or as a function of the values $c_{\max}$ and $c_{\min}$ (abscissa). The different diagrams correspond to different flow directions and different block sizes. The points are closer to the bisector for $c_{\max}$ and $c_{\min}$ than for K_1 and K_2. This indicates that the values $c_{\max}$ and $c_{\min}$ are closer to the reference values than K_1 and K_2.

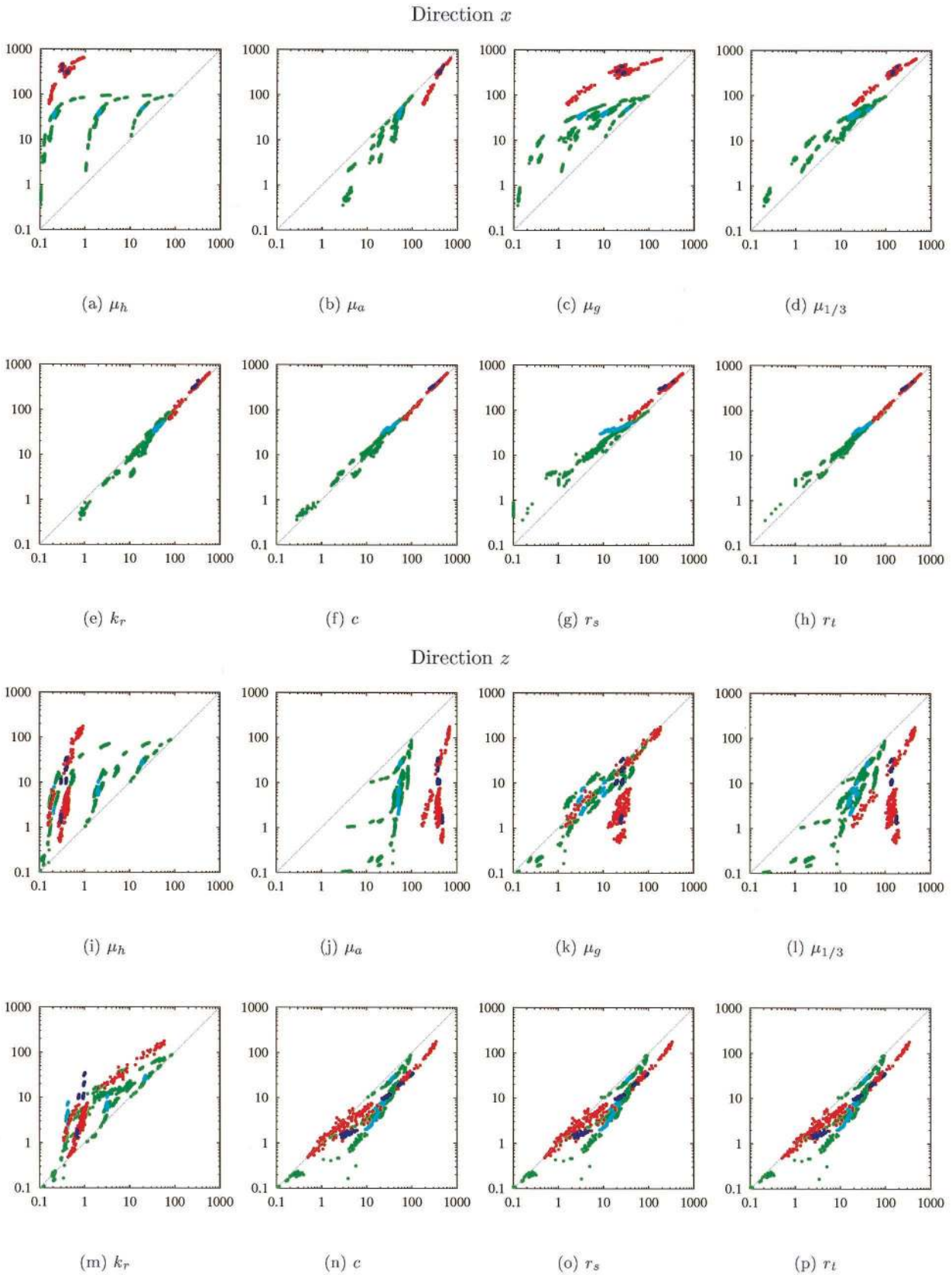

Plate 2. Large blocks. Scatter diagrams of the reference equivalent conductivity (ordinate) as a function of the different fast upscaling techniques (abscissa). Definitions are as follows: μ_h, harmonic mean; μ_a, arithmetic mean; μ_g, geometric mean; $\mu_{1/3}$, Landau-Lifshitz-Matheron conjecture; k_r, Romeu's formula; c, simplified renormalization; r_s, standard renormalization; and r_t, tensorial renormalization.

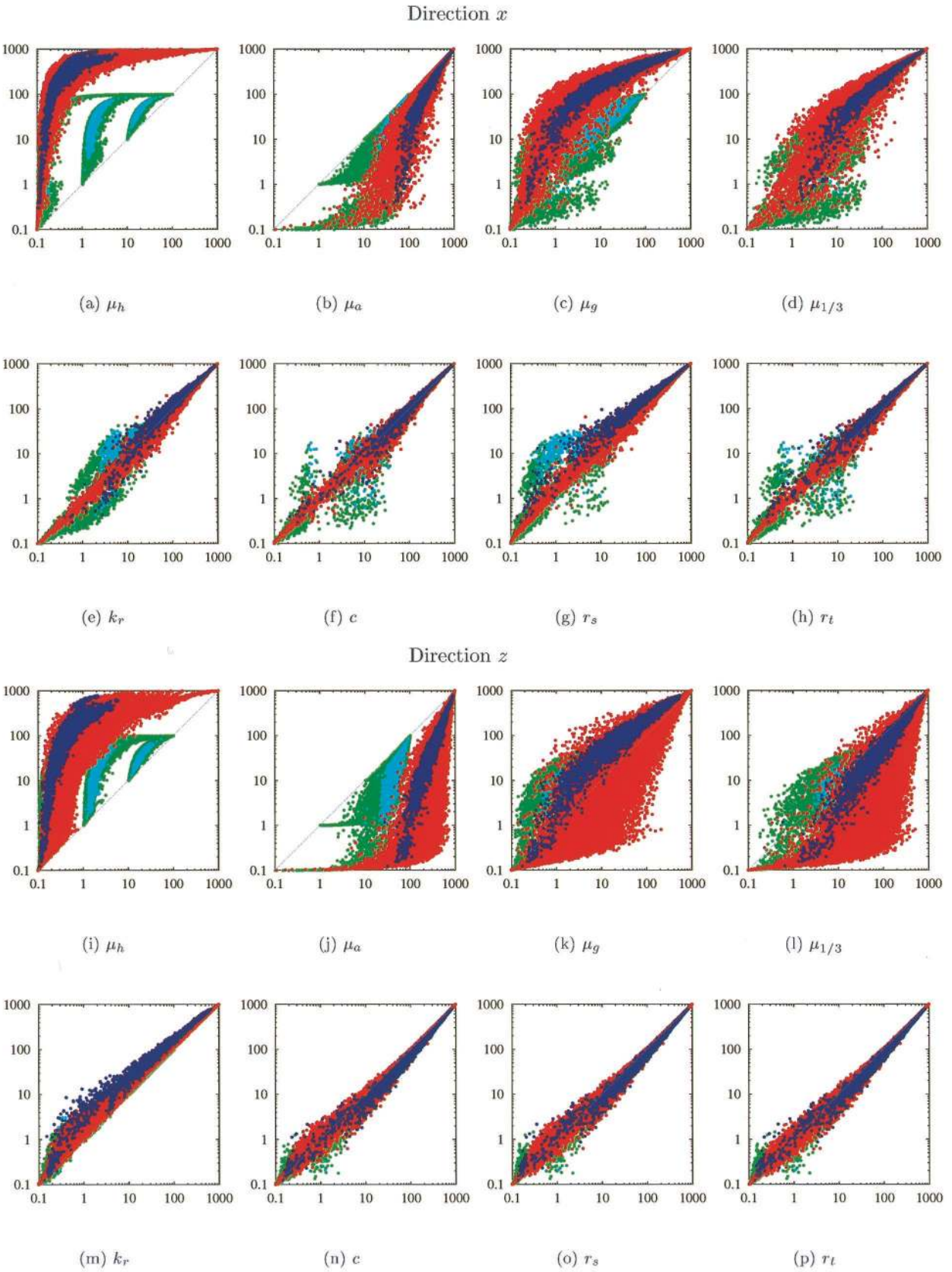

Plate 3. Small blocks. Scatter diagrams of the reference equivalent conductivity (ordinate) as a function of the different fast upscaling techniques (abscissa). Definitions are as follows: μ_h, harmonic mean; μ_a, arithmetic mean; μ_g, geometric mean; $\mu_{1/3}$, Landau-Lifshitz-Matheron conjecture; k_r, Romeu's formula; c, simplified renormalization; r_s, standard renormalization; and r_t, tensorial renormalization.

Table 5. Mean CPU Time in Seconds on a Sparc 10 Workstation[a]

Method	Small Blocks[b] (2,048 cells)	Large Blocks[c] (1,048,576 cells)
Algebraic means	0.04	27
Romeu formula	0.04	42
Simplified renormalization	0.07	49
Tensorial renormalization	0.36	215
Standard renormalization	1.04	445

[a]Input and output are taken into account.
[b]There are 461 finite elements in small blocks.
[c]There are 10,286 finite elements in large blocks.

and is therefore faster. Obviously, the algebraic means are the fastest. The comparison of the execution times for the quick techniques and for the finite elements shows a gain of a factor of between 20 and several hundred.

7. Discussion

7.1. Quality Plots

We observe (Figure 7) a group of techniques corresponding to the renormalization algorithms (r_s, r_t, and c) that have very good linear correlation coefficients and small bias (mostly lower than 10%) and a second group corresponding to the algebraic means (μ_a, μ_g, μ_h, and $\mu_{1/3}$) with smaller linear correlation coefficients. Romeu's formula falls in between. Sometimes it belongs to the first group (for the small blocks experiments); sometimes it belongs to the second (for K_z for the full domains). The algebraic techniques can, in some cases, present a small bias (e.g., μ_g for K_z, see Figures 7b and 7d); however, in general, they present a large dispersion of the estimated conductivity. Among the algebraic techniques the harmonic and the arithmetic means are the least reliable. They can have very strong bias (over 110%) and poor linear correlation coefficients (Figure 7).

7.2. Effect of Block Size and Anisotropy

The differences between Figures 7a–7d show the effects of anisotropy and block size. Concerning the size of the blocks, the accuracy is, in general, better for a small block than for a large one. A rather surprising countercase is the increase in accuracy of the arithmetic mean for K_b^{xx} (compare Figures 7a and 7c). Furthermore, the effect of block size is more important for K_b^{zz} than for K_b^{xx}. Concerning the anisotropy, the accuracy is clearly better for the estimation of the horizontal conductivity than for the vertical one. The worst situation is the estimation of the vertical conductivity of the large blocks. In this case the accuracy of all the techniques is drastically reduced. The relative bias goes from values of less than 5% to values larger than 29% for the best techniques. This effect is more pronounced for k_r (the bias goes from 0.2% for K_b^{xx} in the small blocks to 69.3% for K_b^{zz} in the large blocks). In all cases the techniques that remain closest to the ideal point (upper left-hand corner) are r_s, r_t, and c.

To study the effect of horizontal anisotropy on the techniques, we also compared the classification in the case of Boolean media with ellipsoidal or sinusoidal inclusions (Figures 7e and 7f). With ellipsoidal inclusions the three renormalization techniques and k_r perform well. With sinusoidal inclusions the accuracy of all the techniques deteriorates. The effect is greatest for r_s.

7.3. Limitations of the Renormalization Schemes

In its present formulation the simplified renormalization can handle only regular rectangular grids with a power of 2 number of cells in each direction. The extension to irregular grids requires weighting the local averages by the size of the cells [*Li et al.*, 1999]. The extension to grids that contain a number of cells that are not a power of 2 can follow the procedure proposed by *Hardy and Beier* [1994, p. 210–211] for extending the standard renormalization to these situations.

Again, in its present formulation the simplified renormalization requires the local conductivities to be diagonal. This drawback can be overcome easily by using the exact analytical formulae of *Quintard and Whitaker* [1987, equation 3.36] to aggregate pairs of cells with a full tensor of hydraulic conductivity instead of using the arithmetic and harmonic means. The result will be a full tensor of hydraulic conductivity.

A more important limitation is that the simplified renormalization is not able to detect the principal directions of anisotropy resulting from inclined layers of different conductivities. The consequence is that if the local conductivities are scalar, the upscaled conductivity will be diagonal even if we use the Quintard and Whitaker formula. This results because we work with elementary groups of only two cells. To create such anisotropy, it requires working on elementary groups of at least four cells in two dimensions or eight cells in three dimensions. This is exactly what the tensorial renormalization does, but the cost is a slower algorithm.

Finally, the most important problem that we see is that the simplified renormalization, as well as all the other tested techniques, fails to accurately estimate the vertical conductivity of the large blocks. This kind of inaccuracy was described by *Hardy and Beier* [1994] and by *Malick* [1995] for the standard renormalization. It was interpreted as the result of the accumulation of successive errors in the renormalization procedure due to the use of inadequate permeameter-type boundary conditions on the elementary group of cells. This interpretation is questionable since both the tensorial renormalization, which uses the rather general periodic boundary conditions, and the simplified renormalization, which does not solve a flow problem on the elementary group of cells, are equally inaccurate to estimate the vertical conductivity of the large blocks.

8. Conclusion

A new renormalization technique was devised and intensively tested on two types of heterogeneous synthetic media (truncated Gaussian and Boolean) with high conductivity contrast and strong anisotropy. The numerical experiments showed that among the tested techniques, the two most reliable ones are the tensorial and the new simplified renormalization. Both proved to be more accurate and faster than the original scheme proposed by *King* [1989]. The numerical efficiency of the simplified renormalization (it is about 200 times faster than the finite elements and 4 times faster than the tensorial renormalization) leads us to recommend it when a diagonal tensor of equivalent conductivity is sufficient (when the principal axes of anisotropy are aligned with the axes of the grid). If the nondiagonal terms are required (geological models including cross stratifications, e.g.), we recommend the use of the tensorial renormalization. These two techniques are the best of the techniques we tested; however, they are not always accurate. They give very good results for the horizontal conductivity of the large blocks and for the horizontal and vertical

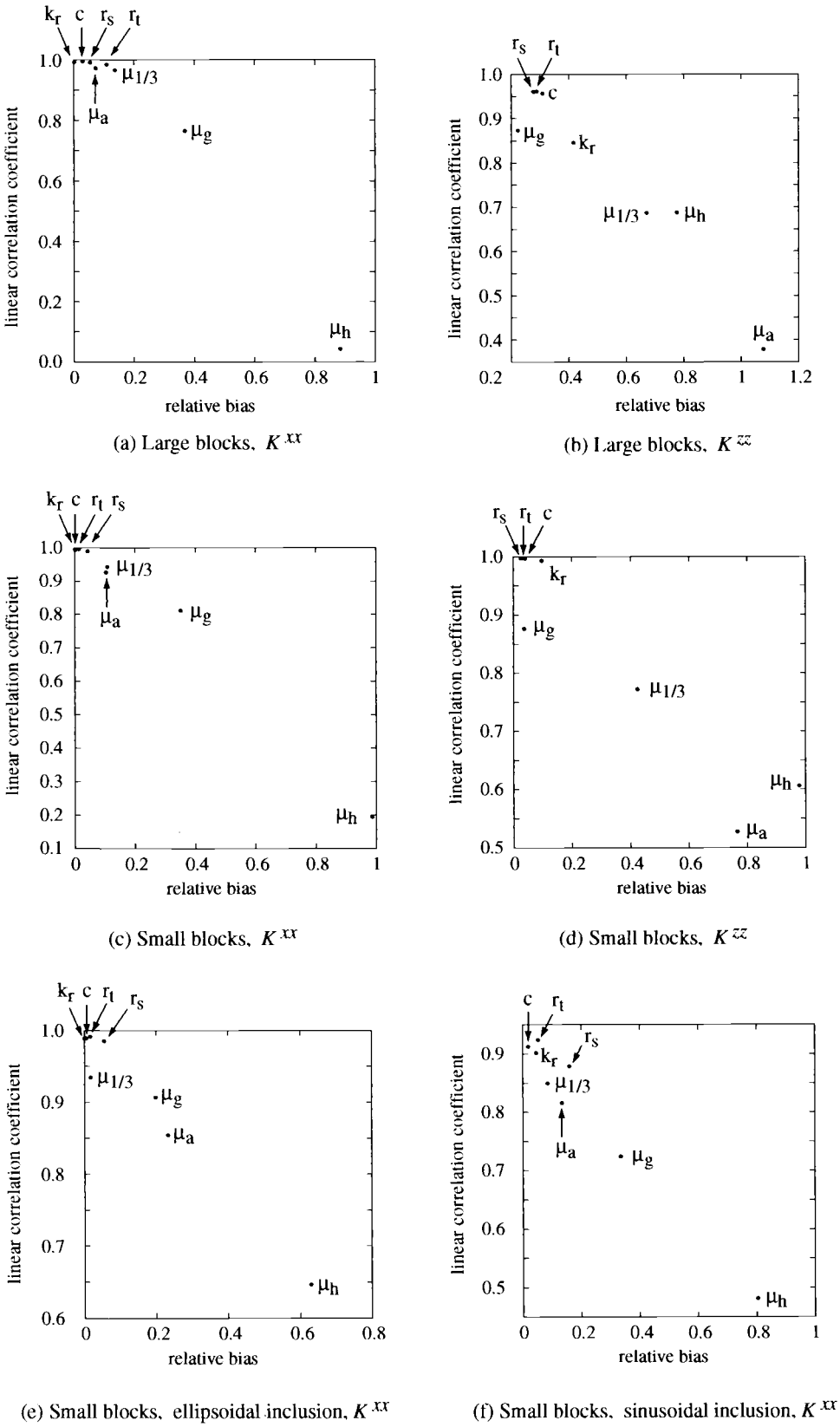

(a) Large blocks, K^{xx}

(b) Large blocks, K^{zz}

(c) Small blocks, K^{xx}

(d) Small blocks, K^{zz}

(e) Small blocks, ellipsoidal inclusion, K^{xx}

(f) Small blocks, sinusoidal inclusion, K^{xx}

Figure 7. Quality plots for the different flow directions and block sizes. The closer the point is to the upper left corner, the better the technique is. Note that the scales and ranges are not identical in all the plots.

conductivity of the small blocks, but they give inaccurate estimations of the vertical conductivity of the large blocks. Additional research is required to develop fast spatial averaging techniques capable of handling such situations.

An important additional result is the demonstration that even if the algebraic techniques (geometric mean, arithmetic mean, etc.) can be almost unbiased for certain types of media, they always show a large dispersion of the estimated values around the reference values. This is due to the fact that they do not take into account the spatial arrangement of the local conductivities. A justification for using them would be to calculate block conductivity when the spatial distribution is completely unknown. The computed results are available to the scientific community on request to allow further research and other comparisons with new upscaling procedures.

Acknowledgments. This work was supported by the Geoscience 2, Reservoir Engineering Project funded by the commission of the European Communities. The manuscript was greatly improved by review comments from R. W. Zimmerman, S. A. Miller, and an anonymous reviewer.

References

Ababou, R., D. McLaughlin, L. W. Gelhar, and A. F. B. Tompson, Numerical simulation of three-dimensional saturated flow in randomly heterogeneous porous media, *Transp. Porous Media*, *4*, 549–565, 1989.

Abramovich, B., and P. Indelman, Effective permeability of log-normal isotropic random media, *J. Phys. A Math. Gen*., *28*, 693–700, 1995.

Aharony, A., E. L. Hinrichsen, A. Hansen, J. Feder, T. Jøssang, and H. H. Hardy, Effective renormalization group algorithm for transport in oil reservoirs, *Physica A*, *177*, 260–266, 1991.

Bachu, S., and D. Cuthiell, Effects of core-scale heterogeneity on steady state and transient fluid flow in porous media: Numerical analysis, *Water Resour. Res*., *26*(5), 863–874, 1990.

Bernasconi, J., Real-space renormalization of bond-disordered conductances lattices, *Phys. Rev. B Condens. Matter*, *18*(5), 2185–2191, 1978.

Cardwell, W. T., and R. L. Parsons, Average permeabilities of heterogeneous oil sands, *Trans. Am. Inst. Min. Metall. Pet. Eng*., *160*, 34–42, 1945.

Dagan, G., *Flow and Transport in Porous Formations*, Springer-Verlag, New York, 1989.

Dagan, G., High-order correction of effective permeability of heterogeneous isotropic formations of lognormal conductivity distribution, *Transp. Porous Media*, *12*, 279–290, 1993.

de Marsily, G., F. Delay, V. Teles, and M. T. Schafmeister, Some current methods to represent the heterogeneity of natural media in hydrogeology, *Hydrogeol. J*., *6*, 115–130, 1998.

Desbarats, A. J., Numerical estimation of effective permeability in sand-shale formations, *Water Resour. Res*., *23*(2), 273–286, 1987.

Desbarats, A. J., Spatial averaging of hydraulic conductivity in three-dimensional heterogeneous porous media, *Math. Geol*., *24*(3), 249–267, 1992.

Deutsch, C. V., Calculating effective absolute permeability in sandstone/shale sequences, *SPE Form. Eval*., *4*(3), 343–348, 1989.

De Wit, A., Correlation structure dependence of the effective permeability of heterogeneous porous media, *Phys. Fluids*, *7*(11), 2553–2562, 1995.

Duquerroix, J.-P. L., P. Lemouzy, B. Nœtinger, and R. K. Romeu, Influence of the permeability anisotropy ratio on large-scale properties of heterogeneous reservoirs, SPE 26648 paper presented at 68th Annual Technical Conference and Exhibition of the SPE, Houston, Tex., 1993.

Dykaar, B. B., and P. K. Kitanidis, Determination of the effective hydraulic conductivity for heterogeneous porous media using a numerical spectral approach, 2, Results, *Water Resour. Res*., *28*(4), 1167–1178, 1992.

Gautier, Y., and B. Nœtinger, Preferential flow-paths detection for heterogeneous reservoirs using a new renormalization technique, *Transp. Porous Media*, *26*, 1–23, 1997.

Gavrilenko, P., and Y. Guéguen, Flow in fractured media: A modified renormalization method, *Water Resour. Res*., *34*(2), 177–191, 1998.

Gelhar, L. W., and C. L. Axness, Three-dimensional stochastic analysis of macrodispersion in aquifers, *Water Resour. Res*., *19*(1), 161–180, 1983.

Goblet, P., Programme metis 7, Application d'une technique d'éléments finis multigrille à la modélisation d'un milieu fortement hétérogène, *Tech. Rep. LHM/RD/92/2*, École des Mines de Paris-Centr. d'Inform. Géol., Fontainebleau, France, 1992.

Gómez-Hernández, J. J., A stochastic approach to the simulation of block conductivity fields conditioned upon data measured at a smaller scale, Ph.D. dissertation, Stanford Univ., Stanford, Calif., 1991.

Gutjahr, A. L., L. W. Gelhar, A. A. Bakr, and J. R. McMillan, Stochastic analysis of spatial variability in subsurface flows, 2, Evaluation and application, *Water Resour. Res*., *14*(5), 953–959, 1978.

Haldorsen, H. H., and E. Damsleth, Stochastic modeling, *JPT J. Pet. Technol*., *42*, 404–412, 1990.

Hansen, A., S. Roux, A. Aharony, J. Feder, T. Jossang, and H. H. Hardy, Real space renormalization estimates for two-phase flow in porous media, *Transp. Porous Media*, *29*, 247–279, 1997.

Hardy, H. H., and R. A. Beier, *Fractals in Reservoir Engineering*, 359 pp., World Sci., River Edge, N. J., 1994.

Hinrichsen, E. L., A. Aharony, J. Feder, A. Hansen, T. Jøssang, and H. H. Hardy, A fast algorithm for estimating large-scale permeabilities of correlated anisotropic media, *Transp. Porous Media*, *12*, 55–72, 1993.

Jaekel, U., and H. Vereecken, Renormalization group analysis of macrodispersion in a directed random flow, *Water Resour. Res*., *33*(10), 2287–2299, 1997.

King, P. R., The use of field theoretic methods for the study of flow in heterogeneous porous medium, *J. Phys. A Math. Gen*., *20*, 3935–3947, 1987.

King, P. R., The use of renormalization for calculating effective permeability, *Transp. Porous Media*, *4*, 37–58, 1989.

King, P., A. Muggeridge, and W. Price, Renormalization calculations of immiscible flow, *Transp. Porous Media*, *12*, 237–260, 1993.

Koltermann, C. E., and S. M. Gorelick, Heterogeneity in sedimentary deposits: A review of structure-imitating, process-imitating, and descriptive approaches, *Water Resour. Res*., *32*(9), 2617–2658, 1996.

Kozlov, S. M., Central limit theorem for multiscaled permeability, in *Proceedings of Oberwolfach Porous Media Meeting*, Birkhäuser Boston, Cambridge, Mass., 1993.

Lachassagne, P., E. Ledoux, and G. de Marsily, Two-dimensional stochastic modeling of flow in non-uniform confined aquifers: Correction of the systematic bias introduced by numerical models when they are used stochastically, in *2nd European Conference on the Mathematics of Oil Recovery, Arles, France*, edited by D. Guérillot and O. Guillon, pp. 283–286, Technip, Paris, 1990.

Landau, L. D., and E. M. Lifshitz, *Electrodynamics of Continuous Media*, Pergamon, Tarrytown, N. Y., 1960.

Le Loc'h, G., Étude de la composition des perméabilités par des méthodes variationnelles, Ph.D. dissertation, Ecole Natl. Supér. des Mines de Paris, 1987.

Lemouzy, P., Calcul de la perméabilité absolue effective, *Tech. Rep. RF40 2685*, Inst. Fr. du Pét., Paris, 1991.

Li, D., B. Beckner, and A. Kumar, A new efficient averaging technique for scaleup of multimillion-cell geologic models, SPE 56554 paper presented at 74th Annual Technical Conference and Exhibition of the SPE, Houston, Tex., 1999.

Malick, K. M., Boundary effects in the successive upscaling of absolute permeability, Master's thesis, Stanford Univ., Stanford, Calif., 1995.

Matheron, G., *Eléments Pour une Théorie des Milieux Poreux*, Masson, Paris, 1967.

Matheron, G., H. Beucher, C. de Fouquet, A. Galli, D. Guérillot, and C. Ravenne, Conditional simulation of the geometry of fluvio-deltaic reservoirs, SPE 16753 paper presented at 62nd Annual Technical Conference and Exhibition of the SPE, Dallas, Tex., 1987.

McCarthy, J. F., Comparison of fast algorithms for estimating large-scale permeabilities of heterogeneous media, *Transp. Porous Media*, *19*, 123–137, 1995.

Meier, P. M., J. Carrera, and X. Sánchez-Vila, An evaluation of Jacob's method for the interpretation of pumping tests in heterogeneous formations, *Water Resour. Res*., *34*(5), 1011–1025, 1998.

Neuman, S. P., and S. Orr, Prediction of steady state flow in nonuniform geologic media by conditional moments: Exact nonlocal formalism, effective conductivities and weak approximation, *Water Resour. Res*., *29*(2), 341–364, 1993.

Nœtinger, B., The effective permeability of a heterogeneous porous medium, *Transp. Porous Media*, *15*, 99–127, 1994.

Pozdniakov, S., and C.-F. Tsang, A semianalytical approach to spatial averaging of hydraulic conductivity, *J. Hydrol.*, *216*(1–2), 78–98, 1999.

Quintard, M., and S. Whitaker, Ecoulement monophasique en milieu poreux: Effets des hétérogénéités locales, *J. Méc. Théor. Appl.*, *6*(5), 691–726, 1987.

Renard, P., Modélisation des écoulements en milieux poreux hétérogènes, Calcul des perméabilités équivalentes, Ph.D. dissertation, Ecole Natl. Supér. des Mines de Paris, 1997.

Renard, P., and G. de Marsily, Calculating equivalent permeability: A review, *Adv. Water Resour.*, *20*(5–6), 253–278, 1997.

Reynolds, P., W. Klein, and H. Stanley, A real-space renormalization group for site and bond percolation, *J. Phys. C Solid State Phys.*, *10*, L167–L172, 1977.

Romeu, R. K., Écoulement en milieu hétérogène: Prise de moyenne de perméabilité en régimes permanent et transitoire, Ph.D. dissertation, Univ. Paris VI, Paris, 1994.

Romeu, R. K., and B. Nœtinger, Calculation of internodal transmissivities in finite difference models of flow in heterogeneous porous media, *Water Resour. Res.*, *31*(4), 943–959, 1995.

Sànchez-Vila, X., J. P. Girardi, and J. Carrera, A synthesis of approaches to upscaling of hydraulic conductivities, *Water Resour. Res.*, *31*(4), 867–882, 1995.

Saucier, A., Scaling of the effective permeability in multifractal porous media, *J. Phys. A Math. Gen.*, *191*, 289–294, 1992.

Shah, N., and J. M. Ottino, Effective transport properties of disordered, multiphase composites: Application of real-space renormalization group theory, *Chem. Eng. Sci.*, *41*(2), 283–296, 1986.

Teodorovich, E., Calculation of the effective permeability of a randomly inhomogeneous porous medium, *J. Exp. Theor. Phys.*, *85*(1), 173–178, 1997.

Warren, J., and H. Price, Flow in heterogeneous porous media, *SPE J.*, *1*, 153–169, 1961.

Wen, X.-H., and J. J. Gómez-Hernández, Upscaling hydraulic conductivities in heterogeneous media: An overview, *J. Hydrol.*, *183*(1–2), ix–xxii, 1996.

Wiener, O., Die Theorie des Mischkörpers für das Feld der stationären Strömung, *Abh. Math. Phys. Klasse Königlichen Sächsischen Ges. Wiss.*, *32*(6), 509–604, 1912.

Wilson, K. G., Renormalization group and critical phenomena, *Phys. Rev. B Condens. Matter.*, *4*(9), 3174–3203, 1971.

Wilson, K. G., The renormalization group: Critical phenomena and the Kondo problem, *Rev. Mod. Phys.*, *47*(4), 773–840, 1975.

Xu, K., J.-F. Daian, and D. Quenard, Multiscale structures to describe porous media, I, Theoretical background and invasion by fluids, *Transp. Porous Media*, *26*, 51–73, 1997.

Zimmerman, R. W., and G. S. Bodvarsson, Effective transmissivity of two-dimensional fracture network, *Int. J. Rock Mech. Min. Sci. Geomech. Abstr.*, *33*(4), 433–438, 1996.

G. de Marsily, Université Pierre et Marie Curie, Laboratoire de Géologie Appliquée, 75252 Paris Cedex 05, France. (GDemarsily@aol.com)

E. Ledoux, Ecole des Mines de Paris, Centre d'Informatique Géologique, 77305 Fontainebleau Cedex, France. (ledoux@cig.ensmp.fr)

G. Le Loc'h, Ecole des Mines de Paris, Centre de Géostatistiques, 77305 Fontainebleau Cedex, France. (leloch@cg.ensmp.fr)

R. Mackay, School of Earth Science, University of Birmingham, Birmingham B15 2TT, England. (R.Mackay@bham.ac.uk)

P. Renard, Swiss Federal Institute of Technology, Institute of Geology, 3093 Zurich, Switzerland. (renard@erdw.ethz.ch)

(Received January 21, 2000; revised May 26, 2000;
accepted July 3, 2000.)